

Article

An Experimental Study on the Large-Volume Liquid Hydrogen Release in an Open Space

Zhao Zhang ¹, Gang Lei ^{1,*}, Ruofan Sun ², Liang Pu ^{1,2}, Tianxiang Wang ¹, Wei Dong ¹, Qiang Chen ¹, Qiufan Wei ¹, Mu Liu ¹, Yongchen He ², Zhi Zheng ¹ and Shengqi Zhang ²

¹ State Key Laboratory of Technologies in Space Cryogenic Propellants, Beijing 100028, China; chan1629@163.com (Q.C.)

² School of Energy and Power Engineering, Xi'an Jiaotong University, Xi'an 710049, China; sunruofan1995@163.com (R.S.); heyongch@126.com (Y.H.)

* Correspondence: leigang_1973@sina.com

Abstract: Liquid hydrogen is one of the high-quality energy carriers, but a large leak of liquid hydrogen can pose significant safety risks. Understanding its diffusion law after accidental leakage is an important issue for the safe utilization of hydrogen energy. In this paper, a series of open-space large-volume liquid hydrogen release experiments are performed to observe the evolution of visible clouds during the release, and an array of hydrogen concentration sensors is set up to monitor the fluctuation in hydrogen concentration at different locations. Based on the experimental conditions, the diffusion of hydrogen clouds in the atmosphere under different release hole diameters and different ground materials is compared. The results show that with the release of liquid hydrogen, the white visible cloud formed by air condensation or solidification is generated rapidly and spread widely, and the visible cloud is most obvious near the ground. With the termination of liquid hydrogen release, solid air is deposited on the ground, and the visible clouds gradually shrink from the far field to the release source. Hydrogen concentration fluctuations in the far field in the case of the cobblestone ground are more dependent on spontaneous diffusion by the hydrogen concentration gradient. In addition, compared with the concrete ground, the cobblestone ground has greater resistance to liquid hydrogen extension; the diffusion of hydrogen clouds to the far field lags. The rapid increase stage of hydrogen concentration at N8 in Test 7 lags about 3 s behind N12 in Test 6, N3 lags about 7.5 s behind N1, and N16 lags about 8.25 s behind N14. The near-source space is prone to high-concentration hydrogen clouds. The duration of the high-concentration hydrogen cloud at N12 is about 15 s, which is twice as long as the duration at N8, increasing the safety risk of the near-source space.

Keywords: experimental study; liquid hydrogen release; diffusion; hydrogen concentration; sensors



Citation: Zhang, Z.; Lei, G.; Sun, R.; Pu, L.; Wang, T.; Dong, W.; Chen, Q.; Wei, Q.; Liu, M.; He, Y.; et al. An Experimental Study on the Large-Volume Liquid Hydrogen Release in an Open Space. *Appl. Sci.* **2024**, *14*, 3645. <https://doi.org/10.3390/app14093645>

Academic Editor: Oriele Palumbo

Received: 21 March 2024

Revised: 15 April 2024

Accepted: 17 April 2024

Published: 25 April 2024



Copyright: © 2024 by the authors. Licensee MDPI, Basel, Switzerland. This article is an open access article distributed under the terms and conditions of the Creative Commons Attribution (CC BY) license (<https://creativecommons.org/licenses/by/4.0/>).

1. Introduction

Liquid hydrogen is an efficient energy carrier with great potential for application in space exploration, energy production, and civil applications [1–8]. However, liquid hydrogen has extremely low temperature and highly flammable characteristics, which will pose serious safety risks in the case of accidental leakage [9,10]. Application scenarios of liquid hydrogen are generally not in confined spaces but mainly in large areas such as space launch sites, hydrogen liquefaction plants, hydrogen refueling stations, and so on. Such scenarios are characterized by the large volume of liquid hydrogen stored and the unimpeded diffusion of liquid hydrogen after leakage, with the hydrogen cloud formed by the evaporation of liquid hydrogen spontaneously spreading by a concentration gradient or spreading with the wind, resulting in a wide range of flammable and explosion regions.

The diffusion behavior of liquid hydrogen in open or closed spaces has been studied extensively by researchers. In the experiment aspect, the most recognized liquid hydrogen release experiments in the last century were performed by the National Aeronautics and

Space Administration (NASA) at the White Sands Test Facility in New Mexico [11]. In that experiment, about 180 kg of liquid hydrogen was released onto the ground in 38 s, through a release vent with an area of 0.25 m². A fence with a diameter of 9.1 m was built around the release source. An array of sensors was arranged to monitor the dynamic hydrogen concentrations at different locations. According to the captured data, the profile of the hydrogen concentration distribution was obtained, which is widely used to validate the numerical models. Under the effect of ambient wind, the farthest downwind distance and the farthest downwind height of the flammable cloud reached 157.5 m and 63.9 m, respectively. The visible cloud survived for 90 s. In this century, the Health and Safety Laboratory (HSL) carried out large-scale LH₂ release experiments [12]. The release rate was 0.07 kg/s from a hole with a diameter of 26.6 mm, and the release direction included horizontal and vertical. The experiment mainly found that once the substrate contacted with liquid hydrogen was cooled enough, the liquid hydrogen pool formed, and solid air appeared.

Considering the flammability and explosiveness of hydrogen, liquid nitrogen and liquid helium are good alternatives to liquid hydrogen, which are often chosen by researchers to carry out cryogenic fluid release experiments. Shu et al. [13] designed a series of liquid helium spilling experiments to reveal the dispersion characteristics of liquid hydrogen in a confined space, and the concentration cloud and the infrared cloud images were captured. Nguyen et al. [14] performed an experiment to spill liquid nitrogen onto unbounded ground to evaluate the influence of the release rate on the evaporation rate. The results show that the greater the release rate, the higher the evaporation rate. In addition, they derived an equation to estimate the evaporation rate of the spreading pool through experimental data. They also conducted an experiment to study the vaporization of the bounded cryogenic liquid pool on concrete ground [15]. The dynamic temperature near the ground surface was measured, and then the boiling of the liquid nitrogen pool was analyzed. Shao et al. [16] performed a liquid nitrogen jet experiment to simulate the leakages of liquid hydrogen and liquid natural gas, and the transient heat flux on the concrete surface was calculated using the transfer function method. Baroudi et al. [17] built a refrigerated experimental setup to study the release behavior of liquid CO₂ under shipping conditions. Releases under low-pressure (0.7–0.94 MPa, 223–228 K), medium-pressure (1.34–1.67 MPa, 234–245 K), and high-pressure tests (1.83–2.65 MPa, 249–259 K) were designed and observed. Zhu et al. [18] performed an experiment to release 1.4 tons of liquid methane and obtained the visible clouds during the initial stage, middle stage, and final stage. Based on the experiment, they numerically studied the leakage and diffusion characteristics of liquid methane.

Another popular method to study the evolution of the hydrogen cloud in the atmosphere is numerical simulation [19–21], which can rapidly obtain the diffusion characteristics under different environment conditions [22,23], different space types [24–27], different release states [28–31], and so on. In terms of theoretical study, Shi et al. [32] analyzed the diffusion characteristics of the hydrogen cloud during a liquid hydrogen leakage accident based on the Gaussian diffusion theory. The results show that the wind velocity helps the diffusion of the hydrogen cloud, and the dilution of the hydrogen cloud can be enhanced under higher wind velocities. Shu et al. [33] employed the jet integral model to calculate the diffusion of the hydrogen cloud that arises from the release of liquid hydrogen under a crossflow field, and the buoyant effect was concluded. They found that increasing the crossflow field velocity can inhibit the vertical diffusion of the hydrogen cloud, thus increasing the flammable region owing to a lower central trajectory of the flammable cloud.

Although numerical simulations and theoretical derivations are efficient means to study the leakage and diffusion characteristics of liquid hydrogen, there are often many assumptions in the models, which make it impossible to reflect the real situation. In addition, the use of liquid nitrogen as a substitute for liquid hydrogen in existing experiments can reduce the safety hazard of the experiments, but the huge difference in physical properties makes it difficult to generalize the experimental results to the leakage–diffusion of liquid hydrogen. Only a few release experiments used liquid hydrogen in large spaces to observe the diffusion characteristics directly. In order to reveal the diffusion mechanism

of liquid hydrogen in a large open space and to complement the relative experiments, a series of liquid hydrogen release experiments are carried out outdoors, with the total release volume ranging from 0.5 m³ to 3 m³. Meanwhile, arrays of hydrogen concentration sensors and temperature sensors are set up to monitor and investigate the diffusion of the cryogenic hydrogen clouds formed by the evaporation of liquid hydrogen in an open space, which contributes to the development of safety guidelines, risk assessment protocols, and emergency response strategies.

2. Experiment Introduction

2.1. Experimental Setup

The configuration of the liquid hydrogen release experiment is shown in Figure 1. A tank is suspended on a support frame and can be tilted 135° by a remote traction device (that is, from standing upright with the opening pointing vertically upwards to tilted with the opening sloping downwards at 45°). Liquid hydrogen is released onto the ground from the tank. Two forms of liquid hydrogen release tests were conducted: One where the tank's flange is opened by a remote traction device and the liquid hydrogen is directly poured out. The other type involves liquid hydrogen leaking from a 50 mm or 100 mm leak hole. The leak hole is located near the edge of the flange, so that when pouring, it can ensure that liquid hydrogen completely flows out.



Figure 1. The configurations of the liquid hydrogen release experiment.

An array of hydrogen concentration sensors and temperature sensors at heights 2 m, 8 m, 12 m, and 20 m is set up to monitor the distributions of hydrogen concentrations and temperatures in the atmosphere, as shown in Figures 2 and 3. In this paper, the $+x$ direction is specified from N1 to N3, the $+y$ direction is specified as the jet direction, and the $+z$ direction is specified as perpendicular to the ground upwards; the corresponding coordinates are listed in Tables 1 and 2. The hydrogen concentration sensor and temperature sensor at the same location share the same ID number.

The liquid hydrogen storage tank has an inner diameter of 1600 mm and a height of 2000 mm, with a total volume of 4 m³. Two temperature sensors are arranged on the liquid level indicator rod to accurately determine the liquid hydrogen volume released in each test by adjusting the positions of the temperature sensors, as shown in Figure 4. Another two temperature sensors are installed under the upper flange of the storage tank and will be lifted together with the upper flange when the lid is opened to release the liquid hydrogen. The initial moment of release is taken as the point at which the temperatures of both sensors begin to change.

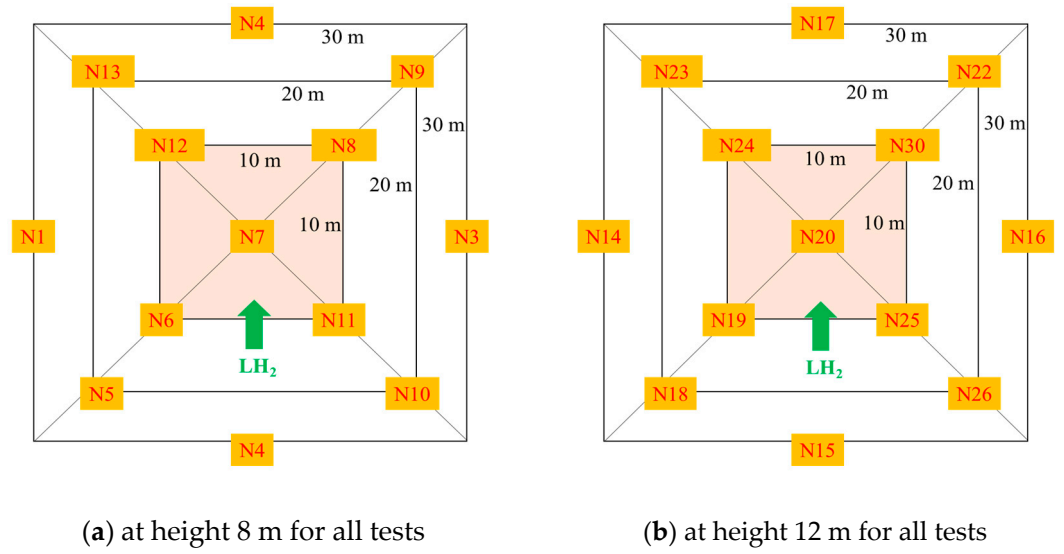


Figure 2. The distributions of the hydrogen concentration sensors at heights 8 m and 12 m.

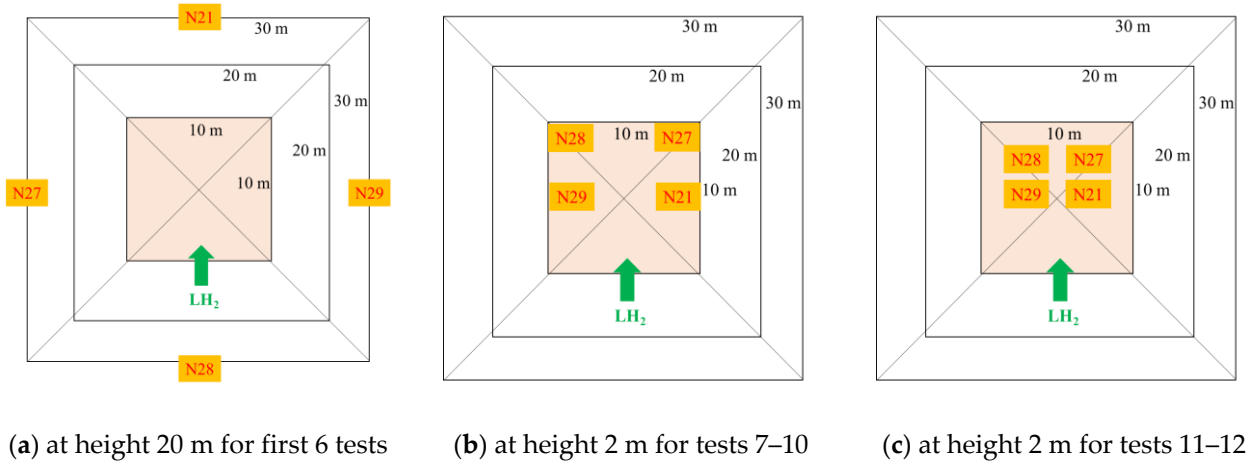


Figure 3. The distributions of the hydrogen concentration sensors at heights 2 m and 20 m.

Table 1. The coordinates of sensors (except sensors N21/T21, N27/T27, N28/T28, and N29/T29).

Sensor ID	x (m)	y (m)	z (m)	Sensor ID	x (m)	y (m)	z (m)	Sensor ID	x (m)	y (m)	z (m)
N1/T1	−15	0	8	N11/T11	5	−5	8	N21/T21	-	-	-
N2/T2	0	−15	8	N12/T12	−5	5	8	N22/T22	10	10	12
N3/T3	15	0	8	N13/T13	−10	10	8	N23/T23	−10	10	12
N4/T4	0	15	8	N14/T14	−15	0	12	N24/T24	−5	5	12
N5/T5	−10	−10	8	N15/T15	0	−15	12	N25/T25	5	−5	12
N6/T6	−5	−5	8	N16/T16	15	0	12	N26/T26	10	−10	12
N7/T7	0	0	8	N17/T17	0	15	12	N27/T27	-	-	-
N8/T8	5	5	8	N18/T18	−10	−10	12	N28/T28	-	-	-
N9/T9	10	10	8	N19/T19	−5	−5	12	N29/T29	-	-	-
N10/T10	10	−10	8	N20/T20	0	0	12	N30/T30	5	5	12

Table 2. The coordinates of sensors N21/T21, N27/T27, N28/T28, and N29/T29.

Sensor ID	Tests 1–6			Tests 7–10			Tests 11–12		
	x (m)	y (m)	z (m)	x (m)	y (m)	z (m)	x (m)	y (m)	z (m)
N21/T21	0	15	20	4	−0.7	2	2	0	2
N27/T27	−15	0	20	4	3.7	2	2	3	2
N28/T28	0	−15	20	−4	3.7	2	−2	3	2
N29/T29	15	0	20	−4	−0.7	2	−2	0	2

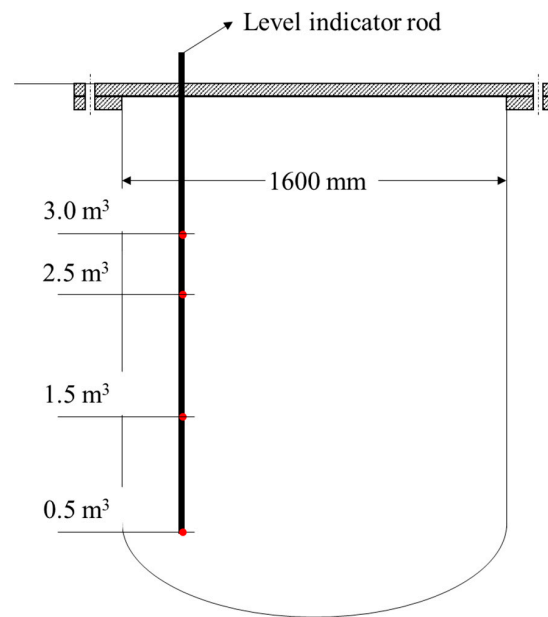


Figure 4. The liquid hydrogen tank with a level indicator rod.

2.2. Test Conditions and Classification

Tables 3 and 4 summarize the release conditions and environmental conditions for the first six tests and the second six tests, respectively. It is worth noting that the first six tests are on concrete grounds, while the last six tests are on cobblestone grounds.

Table 3. The release conditions of liquid hydrogen of the first 6 tests.

Test ID	1	2	3	4	5	6
Release volume (m ³)	0.5	3	3	2	3	2.5
Release duration (s)	-	-	-	-	4	40
Ambient temperature (K)	281.13	293.36	309.15	309.78	291.73	282.54
Relative humidity (%)	26.02	32.24	32.23	33.96	28.83	39.76
Wind velocity (m/s)	0.72	3	0.45	0.68	0.13	0.3
Wind direction to release axis (°)	-	-	-	-	270	45
Release method	Pouring	Pouring	Pouring	Pouring	Pouring	100 mm hole

Table 4. Release conditions of liquid hydrogen of the last 6 tests.

Test ID	7	8	9	10	11	12
Release volume (m ³)	2.5	2.5	1.5	3	3	0.5
Release duration (s)	30	48	25	4	5	20
Ambient temperature (K)	277.76	279.17	283.06	282.05	307.82	307.67
Relative humidity (%)	27.63	29.21	27.46	46.11	79.55	67.13
Wind velocity (m/s)	0.04	0.05	0.61	0.11	0.01	0.15
Wind direction to release axis (°)	135	135	90	270	270	0
Release method	100 mm hole	50 mm hole	50 mm hole	Pouring	Pouring	50 mm hole

The environmental conditions in the above 12 tests are classified to compare specific issues influencing the experimental results. The details are shown in Table 5.

Table 5. Meteorological conditions' classification for liquid hydrogen tests.

Ambient Temperature (°C)	Level	Relative Humidity (%)	Level	Wind Velocity (m/s)	Level
0–20	cold	0–40	dry	0–0.3	No wind
20–30	warm	40–60	moist	0.3–2.5	Gentle wind
30–40	hot	60–100	humid	Above 2.5	High wind

3. Results and Discussion

3.1. Visible Cloud Behaviors during the Release

The images taken in Test 8 are utilized to analyze the visible cloud evolution near the ground and in the environment during and after the liquid hydrogen release.

3.2. Near the Ground

The visible white cloud shown in Figure 5 is formed by the condensation of air's major components (nitrogen, oxygen, water vapor, et al.) encountering liquid hydrogen and cryogenic gaseous hydrogen; among these air components, water vapor has the highest dew point. In Test 8, the relative humidity of the atmosphere is only 30%, and the partial pressure of water vapor is lower than the pressure at the water triple-phase point (611 Pa), so the water vapor converts directly into ice crystals, and the edge of the visible cloud corresponds to the sublimation temperature of water in the current environment. With the release of liquid hydrogen, white visible clouds formed by air condensation or solidification are rapidly generated and widely spread, and the visible clouds are most obvious near the ground.



Figure 5. The visible cloud behaviors during the release near the ground in Test 8.

3.3. In the Atmosphere

The diffusion of visible clouds in the atmosphere is shown in Figure 6. The extent of the cryogenic hydrogen cloud can be qualitatively inferred from the visible cloud distribution, but the edge of the visible cloud is not necessarily the edge of the flammable cloud. Test 8 is in a windless environment, and it can be observed that the visible clouds mainly diffuse in the jet direction while also appearing in the counter-jet direction, which is due to the hydrogen concentration gradient in the atmosphere that makes the cryogenic hydrogen clouds spontaneously diffuse into the surrounding environment. In addition, as the release continues, the size of the visible cloud gradually reaches a steady state.

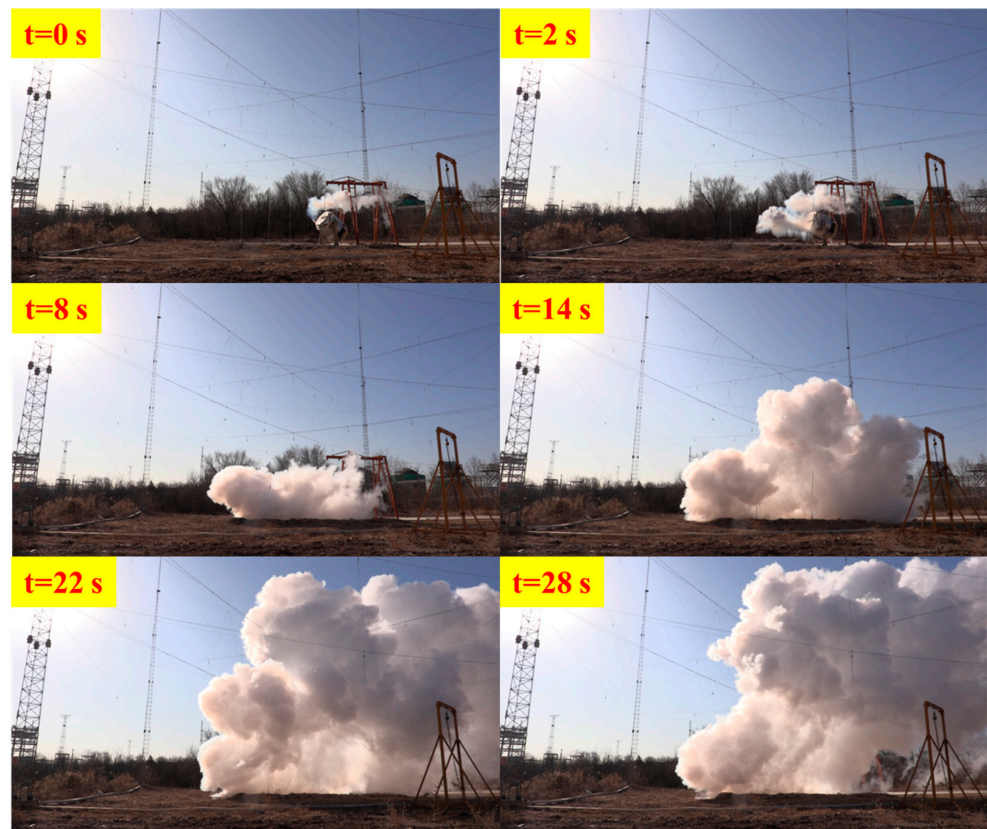


Figure 6. The visible cloud behaviors during the release in the atmosphere in Test 8.

3.4. Visible Cloud Behaviors after Terminating the Release

3.4.1. Near the Ground

Figure 7 shows the evolution of the visible clouds near the ground after terminating the release. Visible clouds shrink back toward the release source, and a small pothole formed by liquid hydrogen collisions is observed on the ground. Here, liquid hydrogen may still exist, and white visible clouds can be observed to arise from the pothole even after terminating the release and spread to the surroundings until the temperature in the pothole returns to ambient temperature.



Figure 7. The visible cloud behaviors after terminating the release near the ground in Test 8.

3.4.2. In the Atmosphere

Figure 8 shows the dissipation of the visible cloud in the atmosphere observed from the far field. The size of the visible cloud evolves from “fat” to “thin”, shrinking from the far field to the release source, rather than fading away vertically from the bottom up.

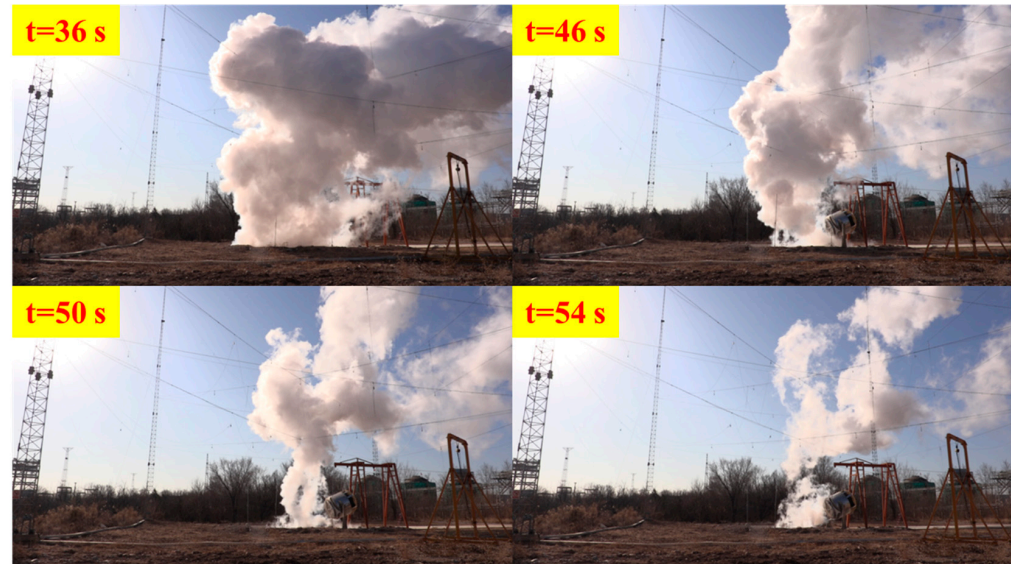


Figure 8. The visible cloud behaviors after terminating the release in the atmosphere in Test 8.

3.5. Effect of Release Conditions

In this section, the diffusions of cryogenic hydrogen clouds under different release hole diameters (Test 7 and Test 8) and different ground materials (Test 6 and Test 7) are studied by analyzing the data from hydrogen concentration sensors and temperature sensors.

3.5.1. Release Hole Diameter

The release hole diameters are 100 mm and 50 mm in Test 7 and Test 8, and it takes 30 s and 60 s for Test 7 and Test 8 to release both 2.5 m³ of liquid hydrogen. The average jet velocity of liquid hydrogen can be calculated by Equation (1):

$$v = \frac{4q}{\pi d^2 t} \quad (1)$$

where v is the jet velocity of liquid hydrogen, q is the total volume of the released liquid hydrogen, d is the hole diameter, and t is the release duration. Therefore, the liquid hydrogen jet velocity in Test 8 is greater than that in Test 7; the diffusion of liquid hydrogen and cryogenic hydrogen clouds is expected to show different behaviors in these two tests. For Test 7, the liquid hydrogen jet velocity is smaller, but the released volume of liquid hydrogen per unit time is larger, so the liquid hydrogen released in Test 7 tends to accumulate on the ground more often compared to Test 8. The sensors that monitored significant hydrogen concentration fluctuations in both tests are N28 and N29 at a height of 2 m and N13 at a height of 8 m, as shown in Figure 9a,b.

The hydrogen concentration fluctuations at sensors N28 and N29 in Test 7 and Test 8 are compared in Figures 10 and 11. Unsurprisingly, the near-source sensors N28 and N29 always monitor the hydrogen concentration fluctuations earlier in Test 8 due to the higher jet velocity. However, when it comes to the far-field sensor N13, the hydrogen concentration fluctuations are monitored in Test 7 about 13 s earlier than in Test 8, as presented in Figure 12.

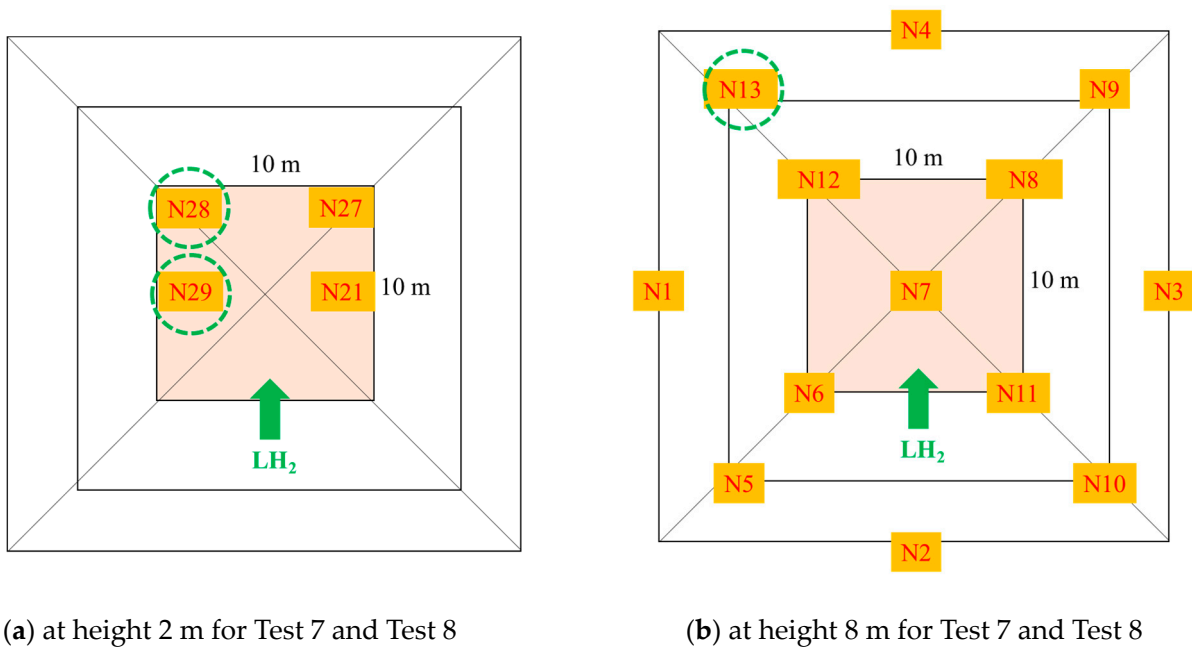


Figure 9. The sensors acquired hydrogen concentration fluctuations at heights 2 m and 8 m.

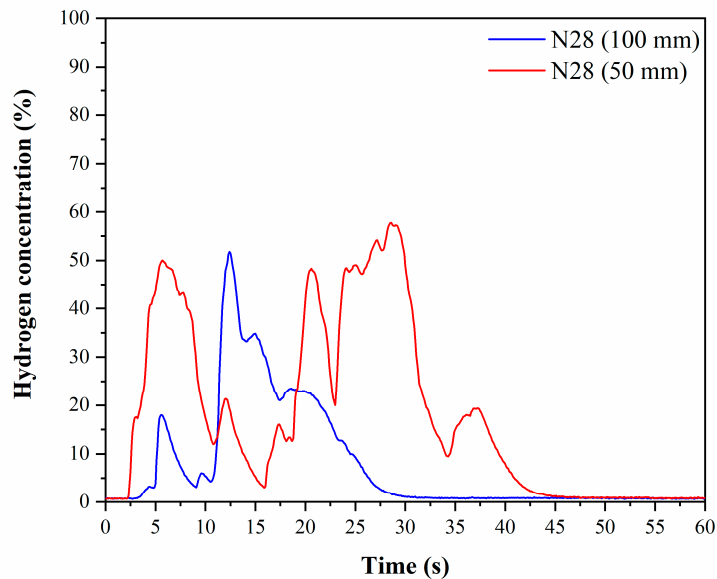


Figure 10. Comparison of hydrogen concentration fluctuations at sensor N28.

In Test 7 and Test 8, the liquid hydrogen pools are almost confined within the cobblestone cover due to the high flow resistance, so the fluctuation in hydrogen concentration at the far-field sensor should be more dependent on spontaneous hydrogen diffusion. As previously mentioned, the liquid hydrogen jet in Test 7 tends to accumulate more on the ground, the near-source concentration of the cryogenic hydrogen cloud is higher, and the temperature difference between the cryogenic hydrogen cloud and the atmosphere is larger, as shown in Figure 13, and therefore the spontaneous hydrogen diffusion will be enhanced, which leads to an earlier monitoring of hydrogen concentration fluctuations in the far-field sensors. In addition, for sensor 13 in Test 7, the temperature here starts to decrease significantly at 5 s, and accordingly, the hydrogen concentration starts to increase dramatically at this point. Similarly in Test 8, at about 18 s, the temperature at sensor 13 begins to decrease and the concentration of hydrogen begins to increase. The results indicate a correlation between hydrogen concentration and temperature fluctuations.

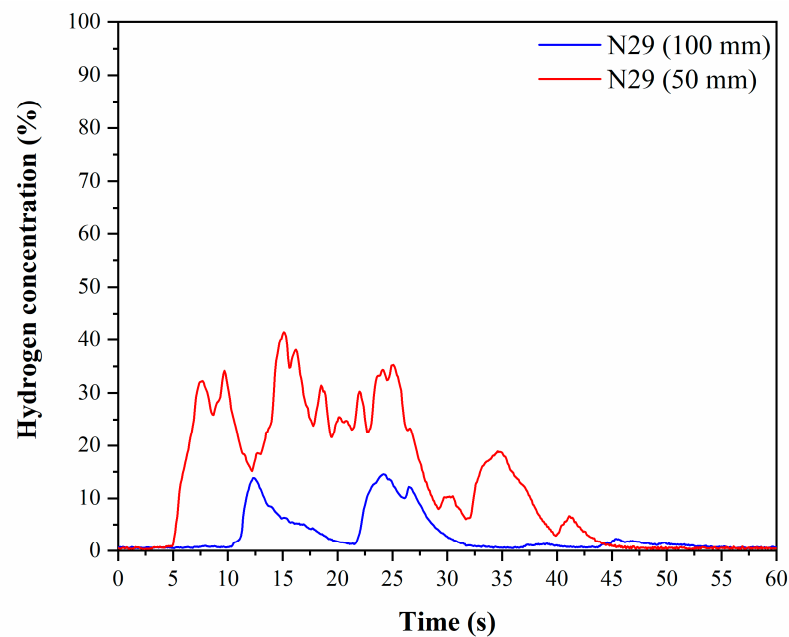


Figure 11. Comparison of hydrogen concentration fluctuations at sensor N29.

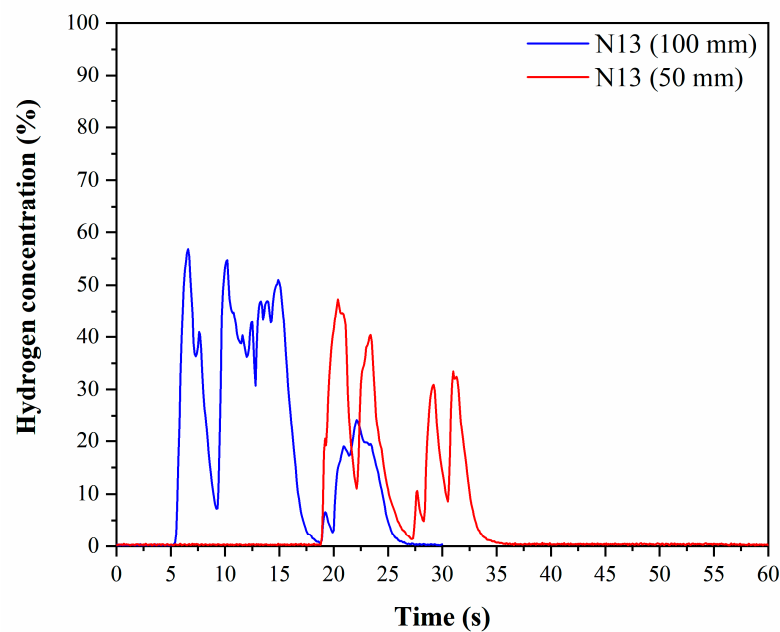


Figure 12. Comparison of hydrogen concentration fluctuations at sensor N13.

3.5.2. Ground Material

The ground material in Test 6 is concrete, while in Test 7, it is cobblestone; all other release and ambient conditions are the same, and the level of wind velocity is no wind (0–0.3 m/s). In Figure 14, it can be observed that the visible cloud is slightly shifted to the right in Test 6 while slightly shifted to the left in Test 7, which could come from a minimal influence of slight ambient wind. Meanwhile, in Test 6, the sensors that monitored significant hydrogen concentration fluctuations are located on the right side of the jet direction (N3, N8, N16), whereas in Test 7, they are located on the left side (N1, N12, N14), as shown in Figure 15. In other words, the sensors that monitored the hydrogen concentration fluctuations in the two tests are symmetric about the y -axis. Therefore, we consider these symmetrical sensors in the same location. The hydrogen concentration fluctuations at these locations in the two tests are investigated to evaluate the effect of the

ground material (concrete or cobblestone) on the diffusion behaviors of the liquid hydrogen and cryogenic hydrogen clouds, as shown in Figures 16–18. The blue curve corresponds to Test 6 (concrete ground), and the red curve corresponds to Test 7 (cobblestone ground).

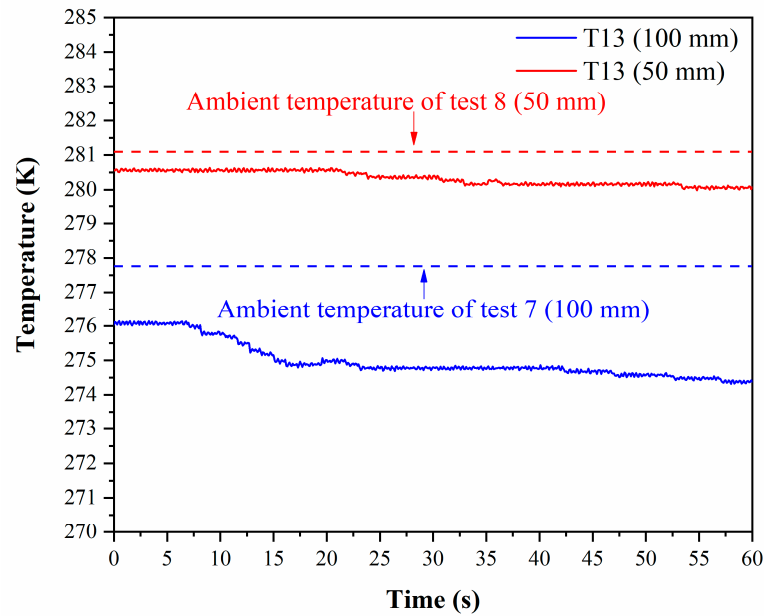


Figure 13. Comparison of temperature fluctuations at sensor T13.



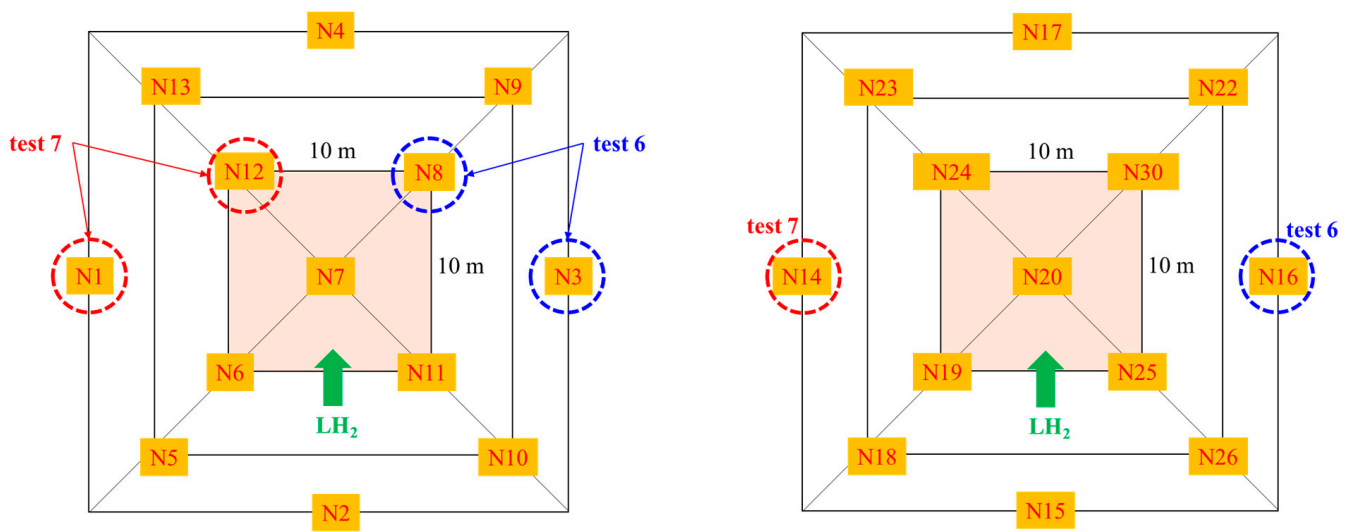
(a) Test 6



(b) Test 7

Figure 14. The liquid hydrogen releases in Test 6 and Test 7.

It can be seen that the sensors in Test 6 all detect the rapid increase stage of the hydrogen concentration much earlier, although the maximum hydrogen concentration is smaller than that in Test 7. It can be inferred that due to the higher resistance to flow on the cobblestone ground in Test 7, the flow of liquid hydrogen is much slower, resulting in a lag in the rapid rise stage of the hydrogen concentration at the sensors. In addition, the farther away the sensors are from the release source, the more significant the lag effect becomes; N8 lags by about 3.0 s compared to N12, N3 lags by about 7.5 s compared to N1, and N16 lags by about 8.3 s compared to N14. On the other hand, the pools of liquid hydrogen on the cobblestone ground tend to accumulate in the near-source regions, thus resulting in a more concentrated cloud of high-concentration hydrogen in Test 7. For example, the maximum hydrogen concentration at N8 in Test 6 is about 25%, whereas at N12 in Test 7, it can be as high as 75%, and the duration of the high-concentration hydrogen cloud at N12 is about 15 s, which is twice as long as the duration at N8. From Figures 17 and 18, it can be seen that the maximum hydrogen concentrations at the sensors with the same x and y coordinates but with a higher height in both tests are lower than those at lower heights, indicating that the higher the height, the higher the dilution of hydrogen clouds.



(a) at height 8 m for Test 6 and Test 7

(b) at height 12 m for Test 6 and Test 7

Figure 15. The sensors acquired hydrogen concentration fluctuations at heights 8 m and 12 m.

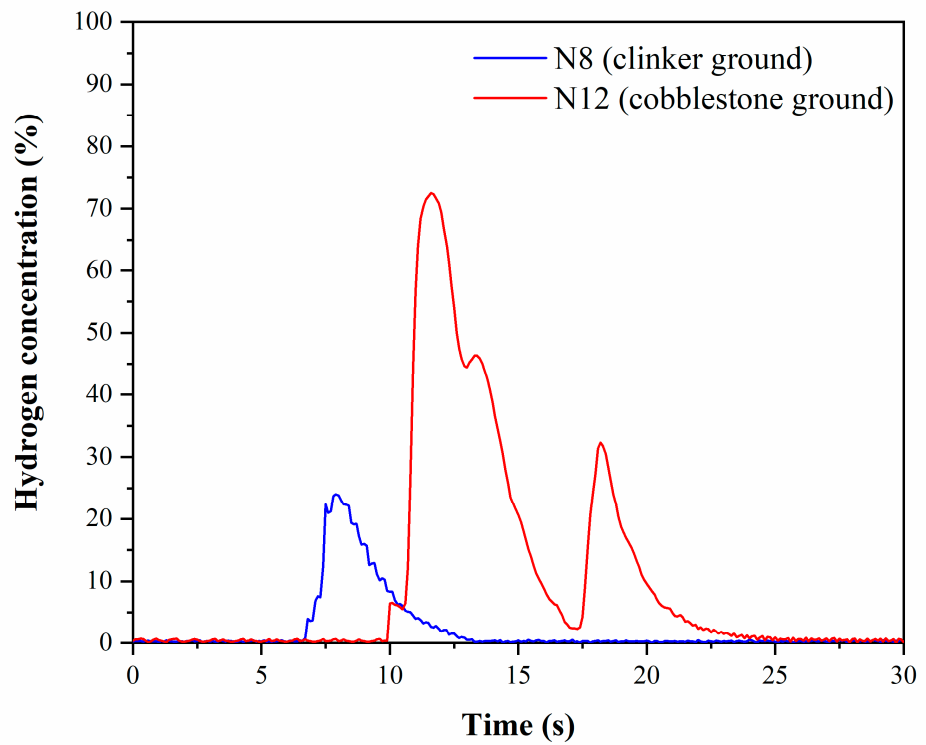


Figure 16. Comparison of hydrogen concentration fluctuations at sensors N8 (Test 6) and N12 (Test 7).

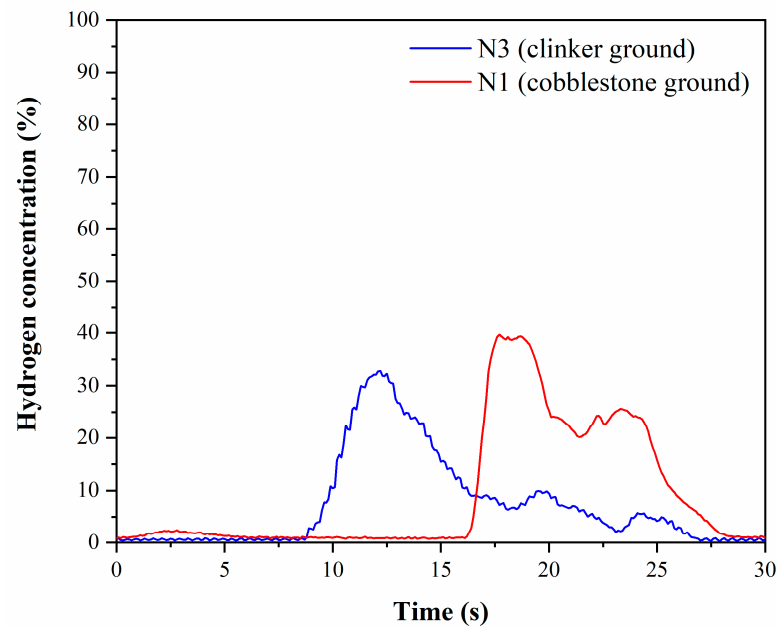


Figure 17. Comparison of hydrogen concentration fluctuations at sensors N3 (Test 6) and N1 (Test 7).

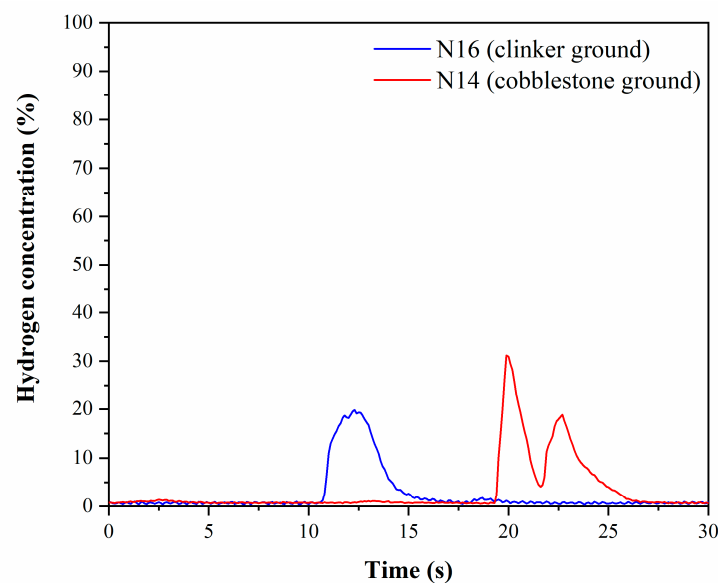


Figure 18. Comparison of hydrogen concentration fluctuations at sensors N16 (Test 6) and N14 (Test 7).

4. Conclusions

In this paper, large-scale liquid hydrogen release experiments were conducted under various release conditions and materials of the ground, and the main conclusions obtained through result analysis can be summarized as follows.

- (1) With the release of liquid hydrogen, white visible clouds formed by the condensation or solidification of air's major components are rapidly generated and widely spread, and the visible clouds are most obvious near the ground. With the end of liquid hydrogen release, solid air is deposited on the ground and the visible cloud gradually shrinks from the far field to the release source.
- (2) Hydrogen concentration fluctuations in the far field in the case of the cobblestone ground are more dependent on spontaneous diffusion by a hydrogen concentration gradient. With a larger diameter of the release hole, liquid hydrogen tends to accumulate on the ground, the heat exchange with the ground deteriorates, the tem-

perature of the hydrogen cloud decreases, convection in the atmosphere becomes more pronounced, and fluctuations in hydrogen concentration in the far field are monitored earlier.

- (3) Compared with the concrete ground, the cobblestone ground has greater resistance to the extension of liquid hydrogen, and the hydrogen cloud diffusion to the far field lags. The rapid increase stage of the hydrogen concentration at N8 in Test 7 lags about 3.0 s behind N12 in Test 6, N3 lags about 7.5 s behind N1, and N16 lags about 8.3 s behind N14. The near-source space is prone to high-concentration hydrogen clouds. The duration of the high-concentration hydrogen cloud at N12 is about 15 s, which is twice as long as the duration at N8 and thus increases the safety risk of the near-source space.

Author Contributions: Methodology, G.L.; Investigation, Z.Z. (Zhao Zhang); Resources, T.W., W.D., Q.C., Q.W., M.L. and Z.Z. (Zhi Zheng); Data curation, Y.H.; Writing—original draft, R.S.; Writing—review & editing, L.P. and S.Z. All authors have read and agreed to the published version of the manuscript.

Funding: This research work is supported by the State Key Laboratory of Technologies in Space Cryogenic Propellants (SKLTSCP202208).

Institutional Review Board Statement: Not applicable.

Informed Consent Statement: Not applicable.

Data Availability Statement: The original contributions presented in the study are included in the article, further inquiries can be directed to the corresponding author.

Conflicts of Interest: The authors declare that they have no known competing financial interests or personal relationships that could have appeared to influence the work reported in this paper.

References

1. Estermann, T.; Newborough, M.; Sterner, M. Power-to-gas systems for absorbing excess solar power in electricity distribution networks. *Int. J. Hydrogen Energy* **2016**, *41*, 13950–13959. [CrossRef]
2. Cheli, L.; Guzzo, G.; Adolfo, D.; Carcasci, C. Steady-state analysis of a natural gas distribution network with hydrogen injection to absorb excess renewable electricity. *Int. J. Hydrogen Energy* **2021**, *46*, 25562–25577. [CrossRef]
3. Nistor, S.; Dave, S.; Fan, Z.; Sooriyabandara, M. Technical and economic analysis of hydrogen refuelling. *Appl. Energy* **2016**, *167*, 211–220. [CrossRef]
4. Okedu, K.E. Hydrogen production using variable and fixed speed wind farm topologies in a utility grid. *J. Renew Sustain. Energy* **2016**, *8*, 1–13. [CrossRef]
5. Dickinson, R.R.; Battye, D.L.; Linton, V.M.; Ashman, P.J.; Nathan, G.J. Alternative carriers for remote renewable energy sources using existing CNG infrastructure. *Int. J. Hydrogen Energy* **2010**, *35*, 1321–1329. [CrossRef]
6. Amoo, L.M.; Fagbenle, R.L. An integrated impact assessment of hydrogen as a future energy carrier in Nigeria's transportation, energy and power sectors. *Int. J. Hydrogen Energy* **2014**, *39*, 12409–12433. [CrossRef]
7. Haeseldonckx, D.; D'haeseleer, W. The use of the natural-gas pipeline infrastructure for hydrogen transport in a changing market structure. *Int. J. Hydrogen Energy* **2007**, *32*, 1381–1386. [CrossRef]
8. Midilli, A.; Dincer, I. Hydrogen as a renewable and sustainable solution in reducing global fossil fuel consumption. *Int. J. Hydrogen Energy* **2008**, *33*, 4209–4222. [CrossRef]
9. Wang, L.; Ma, H.; Shen, Z.; Chen, D. The influence of an orifice plate on the explosion characteristics of hydrogen-methane-air mixtures in a closed vessel. *Fuel* **2019**, *256*, 115908. [CrossRef]
10. Emami, S.D.; Rajabi, M.; Che Hassan, C.R.; Hamid, M.D.A.; Kasmani, R.M.; Mazangi, M. Experimental study on premixed hydrogen/air and hydrogen-methane/air mixtures explosion in 90 degree bend pipeline. *Int. J. Hydrogen Energy* **2013**, *38*, 14115–14120. [CrossRef]
11. Witcofski, R.D.; Chirivella, J.E. Experimental and analytical analyses of the mechanisms governing the dispersion of flammable clouds formed by liquid hydrogen spills. *Int. J. Hydrogen Energy* **1984**, *9*, 425–435. [CrossRef]
12. Hooker, P.; Willoughby, D.B.; Royle, M. Experimental Releases of Liquid Hydrogen. Available online: <https://conference.ing.unipi.it/ichs2011/papers/160.pdf> (accessed on 16 April 2024).
13. Shu, Z.; Lei, G.; Liang, W.; Dai, W.; Lu, F.; Zheng, X.; Qian, H. Experimental investigation of hydrogen dispersion characteristics with liquid helium spills in moist air. *Process Saf. Environ.* **2022**, *162*, 923–931. [CrossRef]
14. Le-Duy, N.; Kim, M.; Choi, B. An experimental investigation of the evaporation of cryogenic-liquid-pool spreading on concrete ground. *Appl. Therm. Eng.* **2017**, *123*, 196–204.

15. Nguyen, L.D.; Kim, M.; Chung, K. Vaporization of the non-spreading cryogenic-liquid pool on the concrete ground. *Int. J. Heat Mass Tran.* **2020**, *163*, 120464. [[CrossRef](#)]
16. Shao, X.; Pu, L.; Tang, X.; Yang, S.; Lei, G.; Li, Y. Experimental study of transient liquid nitrogen jet impingement boiling on concrete surface using inverse conduction problem algorithm. *Process Saf. Environ.* **2021**, *147*, 45–54. [[CrossRef](#)]
17. Al Baroudi, H.; Patchigolla, K.; Thanganadar, D.; Jonnalagadda, K. Experimental study of accidental leakage behaviour of liquid CO₂ under shipping conditions. *Process Saf. Environ.* **2021**, *153*, 439–451. [[CrossRef](#)]
18. Zhu, G.; Guo, X.; Yi, Y.; Tan, W.; Ji, C. Experiment and simulation research of evolution process for LNG leakage and diffusion. *J. Loss Prevent Proc.* **2020**, *64*, 104041. [[CrossRef](#)]
19. Koutsourakis, N.; Venetsanos, A.G.; Bartzis, J.G. LES modelling of hydrogen release and accumulation within a non-ventilated ambient pressure garage using the ADREA-HF CFD code. *Int. J. Hydrogen Energy* **2012**, *37*, 17426–17435. [[CrossRef](#)]
20. Zhang, J.; Delichatsios, M.A.; Venetsanos, A.G. Numerical studies of dispersion and flammable volume of hydrogen in enclosures. *Int. J. Hydrogen Energy* **2010**, *35*, 6431–6437. [[CrossRef](#)]
21. Middha, P.; Ichard, M.; Arntzen, B.J. Validation of CFD modelling of LH2 spread and evaporation against large-scale spill experiments. *Int. J. Hydrogen Energy* **2011**, *36*, 2620–2627. [[CrossRef](#)]
22. Shao, X.; Pu, L.; Li, Q.; Li, Y. Numerical investigation of flammable cloud on liquid hydrogen spill under various weather conditions. *Int. J. Hydrogen Energy* **2018**, *43*, 5249–5260. [[CrossRef](#)]
23. Jin, T.; Liu, Y.; Wei, J.; Zhang, D.; Wang, X.; Lei, G.; Wang, T.; Lan, Y.; Chen, H. Numerical investigation on the dispersion of hydrogen vapor cloud with atmospheric inversion layer. *Int. J. Hydrogen Energy* **2019**, *44*, 23513–23521. [[CrossRef](#)]
24. Jin, T.; Wu, M.; Liu, Y.; Lei, G.; Chen, H.; Lan, Y. CFD modeling and analysis of the influence factors of liquid hydrogen spills in open environment. *Int. J. Hydrogen Energy* **2016**, *42*, 732–739. [[CrossRef](#)]
25. Venetsanos, A.G.; Bartzis, J.G. CFD modeling of large-scale LH2 spills in open environment. *Int. J. Hydrogen Energy* **2007**, *1*, 2171–2177. [[CrossRef](#)]
26. Liu, Y.; Wei, J.; Lei, G.; Lan, Y.; Chen, H.; Gao, X.; Wang, T.; Jin, T. Numerical investigation on the effects of dike around liquid hydrogen source on vapor cloud dispersion. *Int. J. Hydrogen Energy* **2019**, *44*, 5063–5071. [[CrossRef](#)]
27. Giannissi, S.G.; Venetsanos, A.G. Study of key parameters in modeling liquid hydrogen release and dispersion in open environment. *Int. J. Hydrogen Energy* **2018**, *43*, 455–467. [[CrossRef](#)]
28. Giannissi, S.G.; Venetsanos, A.G.; Markatos, N.; Bartzis, J. CFD modeling of hydrogen dispersion under cryogenic release conditions. *Int. J. Hydrogen Energy* **2014**, *39*, 15851–15863. [[CrossRef](#)]
29. Liu, Y.; Wei, J.; Lei, G.; Lan, Y.Q. Dilution of hazardous vapor cloud in liquid hydrogen spill process under different source conditions. *Int. J. Hydrogen Energy* **2018**, *43*, 7643–7651. [[CrossRef](#)]
30. Tang, X.; Pu, L.; Shao, X.; Li, Y.; Wang, X. Dispersion behavior and safety study of liquid hydrogen leakage under different application situations. *Int. J. Hydrogen Energy* **2020**, *45*, 31278–31288. [[CrossRef](#)]
31. Sun, R.; Pu, L.; Yu, H.; Dai, M.; Li, Y. Modeling the diffusion of flammable hydrogen cloud under different liquid hydrogen leakage conditions in a hydrogen refueling station. *Int. J. Hydrogen Energy* **2022**, *47*, 25849–25863. [[CrossRef](#)]
32. Shi, B.; Chen, Y.; Hu, Y.; Wang, Y. Research on Leakage and Diffusion characteristics of Liquid Hydrogen Based on Gaussian Diffusion Model. *J. Phys. Conf. Ser.* **2022**, *2247*, 012004. [[CrossRef](#)]
33. Shu, Z.; Liang, W.; Liu, F.; Lei, G.; Zheng, X.; Qian, H. Diffusion characteristics of liquid hydrogen spills in a crossflow field: Prediction model and experiment. *Appl. Energy* **2022**, *323*, 119617. [[CrossRef](#)]

Disclaimer/Publisher’s Note: The statements, opinions and data contained in all publications are solely those of the individual author(s) and contributor(s) and not of MDPI and/or the editor(s). MDPI and/or the editor(s) disclaim responsibility for any injury to people or property resulting from any ideas, methods, instructions or products referred to in the content.